applied optics

Measuring Stokes parameters by means of unitary operations

ZHI-KUN SU[1,2,*] AND JIA-HUI WANG[1,2]

[1]Guangdong-Hong Kong-Macao Joint Laboratory for Intelligent Micro-Nano Optoelectronic Technology, Foshan University, Foshan 528225, China
[2]School of Physics and Optoelectronic Engineering, Foshan University, Foshan 528225, China
*Corresponding author: suzhikun@163.com

Received 3 August 2021; revised 6 October 2021; accepted 8 October 2021; posted 12 October 2021 (Doc. ID 439420); published 27 October 2021

We propose an improved scheme to measure the Stokes polarization parameters by making the to-be-measured state evolve unitarily. An optical setup able to implement the scheme is presented theoretically and experimentally. Theoretical results indicate that at least two unitary operators should be employed to determine the Stokes parameters of light with arbitrary degrees of polarization. Compared with the results acquired by a commercial polarimeter, the proposed scheme is used to obtain the Stokes parameters of 13 representative states with degrees of polarization $r = 1$ and $r = 0.5$, experimentally. The fidelity between the two states gained by the above methods is in the range of 0.9802 ± 0.0046 to 1.0000 ± 0.0000.

https://doi.org/10.1364/AO.439420

1. INTRODUCTION

The polarization state is one of the freedoms of light, such as intensity, wavelength, frequency, and so on. It is well known that Stokes parameters can be used to characterize all kinds of polarization states of light, not only the fully polarized state. The Stokes polarization parameters are useful because they are directly accessible to measurement. This is due to the fact that they are an intensity formulation of the polarization state of an optical beam [1]. There are a number of methods for measuring Stokes parameters [2–5]. Two excellent methods are mainly referenced in this paper [6,7]. In 2007, Beth *et al.* considered a beam passing through a rotating quarter-wave plate followed by a linear horizontal polarizer, recorded the intensity versus rotating angle and obtained four Stokes parameters from the fitting continuous curve [6]. The quarter-wave plate method is attractive because of its accuracy and simplicity. In 2015, a new method was suggested to apply a pair of cascaded $LiNbO_3$ crystals as a phase retarder in replacing the wave plate, which has the merits of being static without moving elements and rapid measurement [7]. The reason that one needs a pair of cascaded crystals instead of only one crystal is to avoid the influence of the intrinsic phase delay, which changes with temperature and wavelength [7]. Then, one finds that the phase retarder can be regarded as a wave plate with a variable retardation δ and its fast axis at an angle β with the horizontal direction by comparing Eq. (3) in Ref. [7] with Eq. (6.75) in Ref. [8]. The effect on the input state of the phase retarder can be described on the Poincaré sphere, that is, the output state can be obtained from the input state by rotating it clockwise around the diameter in the equatorial plane at an angle 2β with the horizontal direction by an angle δ [8], which is referred to as the effect of a unitary operator hereinafter. The method of using a pair of cascaded $LiNbO_3$ crystals has the merits of being static without moving elements and rapid measurement, but it can be applied to the case with a known polarization degree only when only one unitary operator is operated on the to-be-measured state. In this paper, we use the familiar method from Fourier analysis [6,9] to demonstrate theoretically that at least two unitary operators should be employed to determine the Stokes parameters of any light with arbitrary degrees of polarization (DOPs), that is, one can improve the method of a pair of cascaded crystals [7] by adding one more pair of cascaded crystals. Further, our theory scheme is tested experimentally in an optical setup, in which we realize SU(2) transformations (i.e., unitary operators) using only quarter-wave plates and half-wave plates [10] rather than cascaded crystals. Note that some related works have extended to the quantum domain theoretically [11] and experimentally [12].

The remainder of the paper is organized as follows. Section 2 describes how unitary operators can be used to measure the Stokes parameters. The effect of a unitary operator is reviewed on the Poincaré sphere and an optical experiment to determine the four parameters is suggested as well. Section 3 gives the result of data processing, showing why the scheme proposed in this paper is feasible. The conclusion is given in Section 4.

2. UNITARY OPERATOR METHOD FOR MEASURING STOKES POLARIZATION PARAMETERS

A. Effect of a Unitary Operator on the Poincaré Sphere

Stokes parameters consist of the total intensity S_0 and the three elements of the Stokes vector $\vec{S} = (S_1, S_2, S_3)$, which represent complementary polarization directions on the Poincaré sphere, as shown in Fig. 1(a). The linear polarization states lie on the equator of the sphere, with circular polarization states at the poles. Physically, the three Stokes parameters are obtained from intensity differences between orthogonal polarizations:

$$S_1 = I_{|D\rangle} - I_{|A\rangle}, \quad S_2 = I_{|R\rangle} - I_{|L\rangle}, \quad S_3 = I_{|H\rangle} - I_{|V\rangle}, \tag{1}$$

where subscripts $|H\rangle$, $|V\rangle$, $|D\rangle$, $|A\rangle$, $|R\rangle$ and $|L\rangle$ denote horizontal, vertical, diagonal, anti-diagonal, right circular, and left circular states, respectively. Any polarization state of a light can be represented by

$$\hat{\rho} = \frac{1}{2} S_0 \hat{\sigma}_0 + \frac{1}{2} \vec{S} \cdot \hat{\sigma}, \tag{2}$$

where $\hat{\sigma} = (\hat{\sigma}_1, \hat{\sigma}_2, \hat{\sigma}_3)$, $\hat{\sigma}_0$ being the unit matrix and $\hat{\sigma}_{1,2,3}$ the Pauli matrices

$$\hat{\sigma}_0 \equiv \begin{pmatrix} 1 & 0 \\ 0 & 1 \end{pmatrix}, \quad \hat{\sigma}_1 \equiv \begin{pmatrix} 0 & 1 \\ 1 & 0 \end{pmatrix}, \quad \hat{\sigma}_2 \equiv \begin{pmatrix} 0 & -i \\ i & 0 \end{pmatrix},$$
$$\hat{\sigma}_3 \equiv \begin{pmatrix} 1 & 0 \\ 0 & -1 \end{pmatrix}. \tag{3}$$

Any unitary $U = R_{\vec{n}}(\theta) = \exp(-i\theta \vec{n} \cdot \hat{\sigma}/2)$ operated on the state $\hat{\rho}$ can be considered a rotation on the Poincaré sphere, that is, the tip of the Stokes vector $\vec{S}$ precesses by an angle θ around the axis $\vec{n}$ anticlockwise, when looking at the tip of $\vec{n}$ [13], as shown in Fig. 1(a). Here, we set $\theta \in [0, 2\pi)$. Using the Rodriguez rotation formula [14,15], the initial state $\hat{\rho}$ under the unitary operator becomes

$$\hat{\rho}(\theta) = \exp\left(-i\frac{\theta}{2}\vec{n} \cdot \hat{\sigma}\right) \hat{\rho} \exp\left(i\frac{\theta}{2}\vec{n} \cdot \hat{\sigma}\right)$$
$$= \frac{1}{2} S_0 \hat{\sigma}_0 + \frac{\hat{\sigma}}{2} \cdot [(\vec{S} - \vec{S} \cdot \vec{n}\vec{n}) \cos\theta$$
$$+ (\vec{n} \times \vec{S}) \sin\theta + (\vec{S} \cdot \vec{n})\vec{n}], \tag{4}$$

the derivation process of which is detailed in Appendix A. When $\vec{n}$ lies on the plane of the equator of the Poincaré sphere, i.e., a rotation about a linear polarization with an angle α, the unitary rotation about that axis can be achieved by [16]

$$R_\alpha(\theta) = U_{qwp}\left(\alpha + \frac{\pi}{4}\right) U_{hwp}\left(\alpha - \frac{\pi}{4} - \frac{\theta}{4}\right) U_{qwp}\left(\alpha + \frac{\pi}{4}\right), \tag{5}$$

where U_{qwp} is a quarter-wave plate and U_{hwp} is a half-wave plate. The arguments of the retarders are the angles of their fast axes to the horizontal direction H. Generally, one can use the following wave plate combinations to implement rotation around any axis $\vec{n}$ [16], as shown in Fig. 1(a):

$$R_{\vec{n}}(\theta) = U_{qwp}\left(\frac{\vartheta}{2} + \frac{\pi}{2}\right) R_{\frac{\vartheta}{2}+\frac{\varphi}{2}}(\theta) U_{qwp}\left(\frac{\vartheta}{2}\right), \tag{6}$$

in which $R_{\vartheta/2+\varphi/2}$ can be given by Eq. (5). Next, we will introduce the Poincaré sphere in polar coordinates, as shown in Fig. 1(b). There, the radius of sphere r is defined as

$$r = \frac{\sqrt{S_1^2 + S_2^2 + S_3^2}}{S_0}, \tag{7}$$

where $0 \le r \le 1$ is called the DOP. For completely polarized light, $r = 1$, while for unpolarized light, $r = 0$, and for partially polarized light, $0 < r < 1$. The Stokes parameters of a beam can be written as

$$S_1 = r S_0 \cos(2\varphi) \sin(2\vartheta), \quad S_2 = r S_0 \sin(2\varphi),$$
$$S_3 = r S_0 \cos(2\varphi) \cos(2\vartheta), \tag{8}$$

where $0 \le \vartheta < \pi$ and $-\pi/4 \le \varphi \le \pi/4$ are the azimuth and ellipticity parameters, respectively.

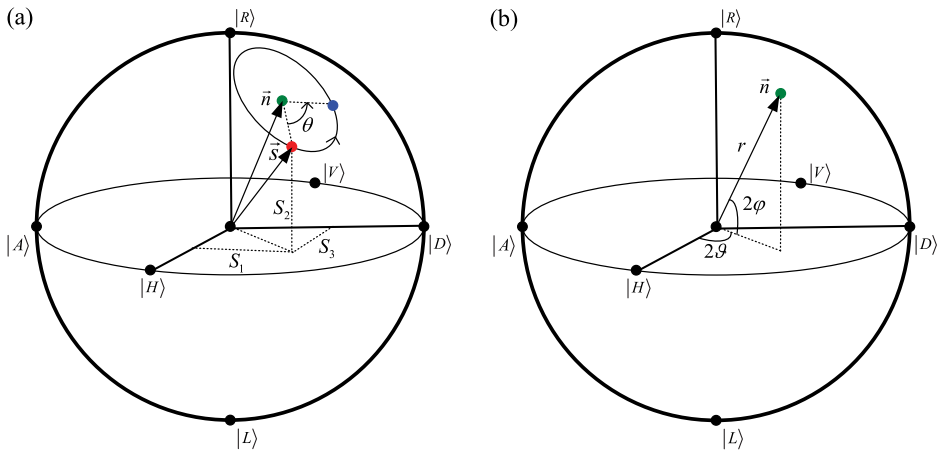

Fig. 1. Poincaré sphere in (a) Cartesian coordinates (S_1, S_2, S_3) and (b) polar coordinates (r, ϑ, φ).

B. Optical Setup

The optical setup is sketched in Fig. 2(a). A linearly polarized He–Ne laser is used as a light source (Melles Griot, model 05-LHP-991, wavelength 632.8 nm, power 7 mW). We first prepare H-polarized light using PBS1 with extinction ratio 10^3, which transmits horizontally polarized light and reflects vertically polarized light. The H-polarized light passes through a quarter-wave plate (Q0 at 45°), leading to right-circular polarization. Then the beam enters a depolarizing module (DM) [17], which is used to control the degree r. With one subsequent half-wave plate (H1 at χ) and one quarter-wave (Q1 at γ), the arbitrary polarization state $\vec{S} = (r S_0 \sin 2\gamma \cos 2[\gamma - 2\chi], r S_0 \sin 2[\gamma - 2\chi], r S_0 \cos 2\gamma \cos 2[\gamma - 2\chi])$ can be prepared. From Eq. (8), one can obtain the azimuth $\vartheta = 2\gamma$ and ellipticity $\varphi = 2(\gamma - 2\chi)$ for the above prepared state in polar coordinates. In brief, any spot on or within the Poincaré sphere can be achieved by properly setting parameters χ, γ, and r.

On the measurement side, we measure an expectation of an observable in state $\hat{\rho}(\theta)$ governed by Eq. (4) to determine the four Stokes parameters S_0, S_1, S_2, S_3 of $\hat{\rho}$ appearing in Eq. (2). The expectation value of an observable $\hat{O}$ can be given as

$$\langle \hat{O} \rangle = \mathrm{Tr}[\hat{\rho}(\theta)\hat{O}]. \tag{9}$$

Letting $\hat{O} = |H\rangle\langle H|$, from Eq. (B1) in Appendix B, Eq. (9) yields

$$\begin{aligned}\langle |H\rangle\langle H| \rangle &= I(\theta) \\ &= \frac{1}{2}S_0 + \frac{1}{2}[S_3 - (S_1 n_1 + S_2 n_2 + S_3 n_3)n_3]\cos\theta \\ &\quad + \frac{1}{2}(n_1 S_2 - n_2 S_1)\sin\theta + \frac{1}{2}(S_1 n_1 + S_2 n_2 + S_3 n_3)n_3,\end{aligned} \tag{10}$$

which is composed of a constant term and two first harmonic terms. It is worth mentioning that Eq. (17) in Ref. [6], different from Eq. (10), is a truncated Fourier series consisting of a constant term, a second harmonic term, and two fourth harmonic terms, which yields four Stokes parameters. However, Eq. (10) indicates that one cannot obtain the four Stokes parameters simultaneously using only one rotation axis $\vec{n}$ unless the to-be-measured state is completely polarized, i.e., $S_0 = \sqrt{S_1^2 + S_2^2 + S_3^2}$. Further, at least two different $\vec{n}$ should be adopted, that is, two unitary U_1 and U_2 should be operated on the initial state given in Eq. (2) if one intends to determine the four Stokes parameters. Experimentally, the expectation value given by Eq. (10) can be realized with the second PBS2 in Fig. 2(a). The two axes, for simplicity, are set from anti-diagonal state $|A\rangle$ to diagonal state $|D\rangle$ (i.e., $n_1 = 1$, $n_2 = 0$, and $n_3 = 0$) and from left circular state $|L\rangle$ to right circular state $|R\rangle$ (i.e., $n_1 = 0$, $n_2 = 1$ and $n_3 = 0$), which can be achieved with the help of retarders [16]; see Fig. 2(b).

3. METHODOLOGY AND RESULT

The optical setup sketched in Fig. 2(a) has been experimentally implemented. All quarter- and half-wave plates used in this setup are mounted to a rotation mount with full 360° engraved scale marked in 2° increments. First, we manually rotate the half-wave plate H2 with 5° a step, which makes the to-be-measured state turn 10° around the axis anticlockwise, and record the intensity accordingly through a power and energy meter (Thorlabs, model PM100USB, with sensor model S120C, wavelength range 400 nm–1100 nm, power range 50 nW–50 mW, resolution 1 nW) for every step from

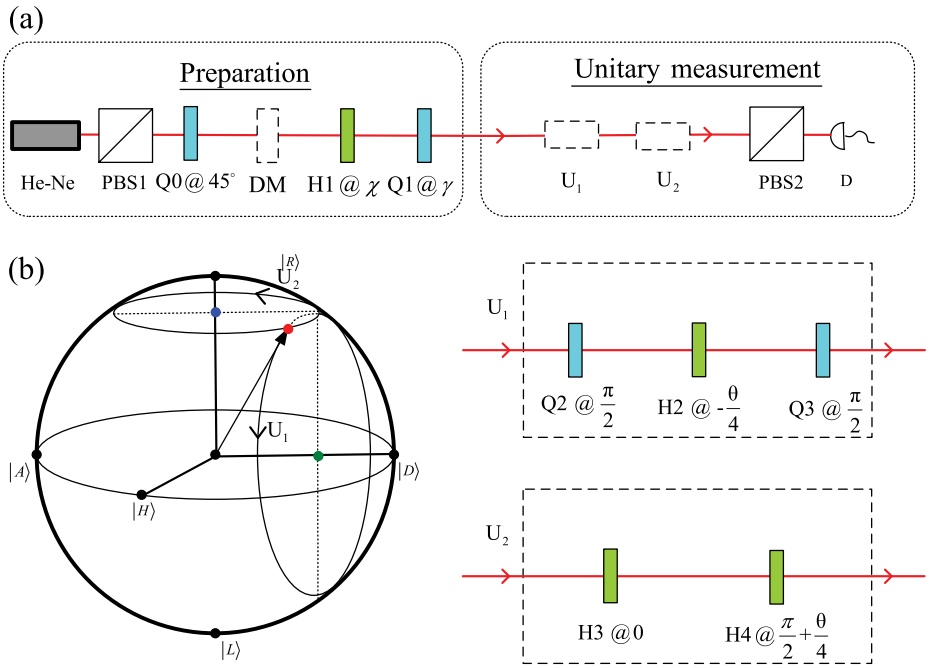

Fig. 2. (a) Setup to measure the Stokes polarization parameters using a single unitary operation. PBS, polarization beam splitter; H, half-wave plate; Q, quarter-wave plate; U, unitary operator; DM, depolarizing module (see Fig. 1 in Ref. [17]). (b) Poincaré sphere to show the effect of unitary operators U_1 and U_2 employed in the experiment. Note that the unitary operator can be realized by the combination of wave plates as well as a pair of cascaded $LiNbO_3$ crystals. Here we use combination of wave plates to operate on the polarized state unitarily.

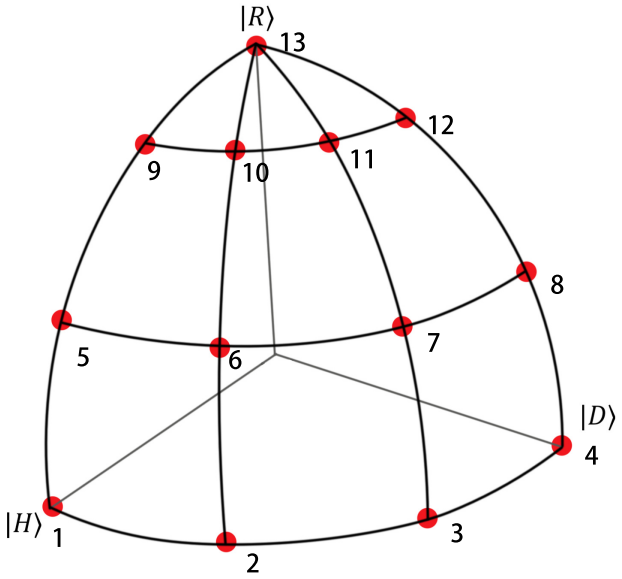

Fig. 3. Thirteen points located on the states to be measured are identified by the red dots, which are evenly distributed over a quarter of the Poincaré sphere. The points are on the surface of the sphere for $r = 1$, while they are on the sphere with 0.5 as its radius for $r = 0.5$ accordingly.

$\theta = 0$ to $\theta = 180°$, that is, 10 data points are measured. Then, the same operation is performed on the half-wave plate H4. Finally, the data consist of intensity versus angle scans, and two discrete curves will be obtained for every to-be-measured state. We use the command global fit in Origin to fit the two curves simultaneously [18] and determine the four Stokes parameters with Eq. (10). To test the capability of our scheme, we compare the fitted parameters with those measured by a commercial polarimeter (Thorlabs, model PAX1000VIS/M, wave range 400–700 nm) for 13 representative states [19], as shown in Fig. 3. The measured values, as well as the fidelities F, are shown in Table 1. Fidelity is a measure of distance between quantum states, and here we use it to quantify how big the difference between the measured and targeted Stokes parameters is. The fidelity of states is defined to be

$$F(\rho_t, \rho_m) = (Tr\sqrt{\sqrt{\rho_t}\rho_m\sqrt{\rho_t}})^2, \tag{11}$$

in which ρ_t and ρ_m are related to the two states gained by the polarimeter and two-unitary methods, respectively. Note that the fidelity is bounded between zero and one. If $\rho_t = \rho_m$, $F(\rho_t, \rho_m) = 1$. On other hand, when ρ_t and ρ_m are perfectly distinguishable, $F(\rho_t, \rho_m) = 0$. The closer fidelity gets to one, the less difference between ρ_t and ρ_m.

From Table 1, we can see that the method introduced in this paper is feasible for both $r = 1$ and $r = 0.5$. However, there are errors in fidelity for every state due to the instrument accuracy of the commercial polarimeter, the power and energy meter, and all the devices used in the setup, among which wave plates mainly affect the axes of rotation of unitary operators, and polarizers or polarized beam splitters influence the DOP of

Table 1. Measured Values of Stokes Parameters for 13 States with $r = 1$ and $r = 0.5$

		Polarimeter				Two-Unitary Method				
States		r	S_1	S_2	S_3	r	S_1	S_2	S_3	**Fidelities**
$r = 1$	State 1	0.9990	−0.020	0.000	0.999	0.9973	−0.021	−0.034	0.996	0.9998 ± 0.0009
	State 2	0.9973	0.489	−0.030	0.869	1.0000	0.530	−0.011	0.848	0.9990 ± 0.0021
	State 3	0.9994	0.840	0.010	0.540	0.9900	0.860	0.025	0.490	0.9982 ± 0.0030
	State 4	0.9968	0.996	0.010	0.030	1.0000	0.997	−0.072	−0.005	0.9982 ± 0.0022
	State 5	0.9934	−0.010	0.526	0.843	1.0000	−0.025	0.524	0.851	0.9983 ± 0.0100
	State 6	0.9984	0.410	0.500	0.760	1.0000	0.422	0.540	0.728	0.9992 ± 0.0106
	State 7	0.9974	0.726	0.508	0.458	0.9519	0.734	0.444	0.413	0.9924 ± 0.0026
	State 8	0.9989	0.851	0.521	0.040	0.9776	0.818	0.536	0.006	0.9963 ± 0.0050
	State 9	0.9957	−0.010	0.856	0.508	0.9876	0.022	0.849	0.504	0.9993 ± 0.0021
	State 10	0.9995	0.221	0.884	0.412	1.0000	0.291	0.872	0.393	0.9992 ± 0.0063
	State 11	0.9997	0.408	0.875	0.259	0.9134	0.418	0.782	0.220	0.9802 ± 0.0046
	State 12	0.9998	0.490	0.870	0.040	0.9309	0.416	0.833	−0.022	0.9836 ± 0.0058
	State 13	0.9993	0.010	0.999	0.020	1.0000	0.044	0.999	0.002	0.9996 ± 0.0111
$r = 0.5$	State 1	0.5009	−0.025	0.010	0.500	0.4657	0.004	0.008	0.466	0.9997 ± 0.0002
	State 2	0.5001	0.235	0.030	0.440	0.5655	0.204	−0.112	0.516	0.9964 ± 0.0016
	State 3	0.5012	0.421	0.025	0.271	0.5069	0.435	−0.013	0.259	0.9998 ± 0.0001
	State 4	0.5001	0.499	0.015	0.025	0.4781	0.478	0.005	0.018	0.9999 ± 0.0001
	State 5	0.5000	−0.025	0.274	0.418	0.5741	0.004	0.279	0.502	0.9987 ± 0.0004
	State 6	0.4993	0.200	0.270	0.370	0.4892	0.208	0.225	0.382	0.9997 ± 0.0002
	State 7	0.5007	0.358	0.269	0.224	0.4200	0.298	0.210	0.210	0.9989 ± 0.0003
	State 8	0.5002	0.420	0.270	0.020	0.4776	0.408	0.247	0.020	0.9999 ± 0.0001
	State 9	0.5000	−0.010	0.446	0.226	0.4596	−0.016	0.383	0.253	0.9994 ± 0.0002
	State 10	0.5005	0.105	0.449	0.195	0.4993	0.123	0.441	0.217	0.9999 ± 0.0001
	State 11	0.5007	0.199	0.443	0.120	0.4766	0.203	0.414	0.119	0.9999 ± 0.0001
	State 12	0.4978	0.234	0.439	0.010	0.5089	0.237	0.450	−0.001	1.0000 ± 0.0000
	State 13	0.5007	0.005	0.500	−0.025	0.4248	0.030	0.423	0.025	0.9987 ± 0.0005

the state. The error in fidelity is calculated from the nonlinear curve fit of the statistical error in this paper. The fidelities of the target states (polarimeter) shown in Fig. 3 to the measured states (two-unitary method) are in the range of 0.9802 ± 0.0046 to 1.0000 ± 0.0000.

4. CONCLUSION

In this paper, we have discussed how the Stokes parameters are measured by making the to-be-measured state evolve unitarily. The theoretical derivation shows that at least two unitary operators should be employed to determine the Stokes parameters of light with arbitrary DOPs. The scheme is proved to be feasible experimentally, and the combinations of wave plates instead of LiNbO3 crystals are used to implement unitary operators in the experiment. The result shows that the fidelity between the target (polarimeter) and measured (two-unitary method) states is in the range of 0.9802 ± 0.0046 to 1.0000 ± 0.0000, which gives a guideline to improve the technique based on the electro-optic effect [7]. Future work will include one more pair of cascaded LiNbO3 crystals, with the new pair of crystals having a value of β different from the original cascaded LiNbO3 crystals. (The optical axis of the crystal has an angle of β with a certain axis in the reference coordinates; see Eq. (3) in Ref. [7].) Since the maximum sampling frequency of a commercial polarimeter (Thorlabs, model PAX1000Vis/M) based on the rotating quarter-wave plate technique is 400 Hz while the maximum modulation frequency of a commercial free-space electro-optic modulator (Thorlabs, model EO-PM-NR-C1) is up to 100 MHz, the setup based on crystals will be better than that of a rotating wave plate in terms of sampling rate.

APPENDIX A

By the formulas

$$\begin{aligned}
&(\vec{S}\cdot\hat{\sigma})(\vec{n}\cdot\hat{\sigma}) - (\vec{n}\cdot\hat{\sigma})(\vec{S}\cdot\hat{\sigma}) \\
&= (S_1\hat{\sigma}_1 + S_2\hat{\sigma}_2 + S_3\hat{\sigma}_3)(n_1\hat{\sigma}_1 + n_2\hat{\sigma}_2 + n_3\hat{\sigma}_3) \\
&\quad - (n_1\hat{\sigma}_1 + n_2\hat{\sigma}_2 + n_3\hat{\sigma}_3)(S_1\hat{\sigma}_1 + S_2\hat{\sigma}_2 + S_3\hat{\sigma}_3) \\
&= -(\vec{n}\times\vec{S})\cdot 2i\hat{\sigma} \qquad \textbf{(A1)}
\end{aligned}$$

and

$$\begin{aligned}
&(\vec{n}\cdot\hat{\sigma})(\vec{S}\cdot\hat{\sigma})(\vec{n}\cdot\hat{\sigma}) \\
&= (n_1\hat{\sigma}_1 + n_2\hat{\sigma}_2 + n_3\hat{\sigma}_3)(S_1\hat{\sigma}_1 + S_2\hat{\sigma}_2 + S_3\hat{\sigma}_3) \\
&\quad \times (n_1\hat{\sigma}_1 + n_2\hat{\sigma}_2 + n_3\hat{\sigma}_3) \\
&= 2(\vec{n}\cdot\hat{\sigma})(\vec{n}\cdot\vec{S}) - (\vec{S}\cdot\hat{\sigma}), \qquad \textbf{(A2)}
\end{aligned}$$

one can obtain

$$\begin{aligned}
&e^{-i\theta\vec{n}\cdot\hat{\sigma}}(\vec{S}\cdot\hat{\sigma})e^{i\theta\vec{n}\cdot\hat{\sigma}} \\
&= (\hat{\sigma}_0\cos\theta - i\vec{n}\cdot\hat{\sigma}\sin\theta)(\vec{S}\cdot\hat{\sigma})(\sigma_0\cos\theta + i\vec{n}\cdot\hat{\sigma}\sin\theta) \\
&= (\vec{S}\cdot\hat{\sigma})\cos^2\theta + i(\vec{S}\cdot\hat{\sigma})(\vec{n}\cdot\hat{\sigma})\cos\theta\sin\theta - i(\vec{n}\cdot\hat{\sigma})(\vec{S}\cdot\hat{\sigma}) \\
&\quad \times \cos\theta\sin\theta + (\vec{n}\cdot\hat{\sigma})(\vec{S}\cdot\hat{\sigma})(\vec{n}\cdot\hat{\sigma})\sin^2\theta \\
&= (\vec{S}\cdot\hat{\sigma})\cos^2\theta + (\vec{n}\times\vec{S})\cdot\hat{\sigma}\sin 2\theta \\
&\quad + [2(\vec{n}\cdot\hat{\sigma})(\vec{n}\cdot\vec{S}) - (\vec{S}\cdot\hat{\sigma})]\sin^2\theta \\
&= \hat{\sigma}\cdot[(\vec{S} - \vec{S}\cdot\vec{n}\vec{n})\cos 2\theta + (\vec{n}\times\vec{S})\sin 2\theta + (\vec{S}\cdot\vec{n})\vec{n}]. \qquad \textbf{(A3)}
\end{aligned}$$

Note that $\vec{n} = (n_1, n_2, n_3)$, $(\vec{n}\cdot\vec{n} = 1)$, $\vec{S} = (S_1, S_2, S_3)$, and $\hat{\sigma} = (\hat{\sigma}_1, \hat{\sigma}_2, \hat{\sigma}_3)$.

APPENDIX B

Letting $\hat{O} = |p\rangle\langle p|$, $(p = H, V, D, A, R, L)$, Eq. (9) yields

$$\langle|p\rangle\langle p|\rangle = I(\theta) = \frac{1}{2}(E \pm F\cos\theta \pm G\sin\theta), \qquad \textbf{(B1)}$$

where "+" will be taken when $p = H, D, R$, while "−" if $p = V, A, L$, and the coefficients are

$$E = S_0 + n_q\sum_{m=1}^{3} n_m S_m, \qquad \textbf{(B2)}$$

$$F = S_q - n_q\sum_{m=1}^{3} n_m S_m, \qquad \textbf{(B3)}$$

$$G = n_{1+|q|_3}S_{1+|q+1|_3} - n_{1+|q+1|_3}S_{1+|q|_3}, \ (q = 1, 2, 3), \qquad \textbf{(B4)}$$

where $|a|_b$ means a mod b, and $q = 1$ for $p = D$ or A, $q = 2$ for $p = R$ or L, while $q = 3$ for $p = H$ or V. Here, we should note that Eq. (B1) is a truncated Fourier series consisting of a constant term and two first harmonic terms. To determine E, F, and G, we should set θ into different values and measure the discrete intensities

$$I_k = \frac{1}{2}[E + F\cos(\theta_k) + G\sin(\theta_k)], \ (k = 1, 2, \ldots, K), \qquad \textbf{(B5)}$$

where the number of samplings $K \geq 3$. The coefficients E, F, and G can be determined using the methods from Fourier analysis [6]. Alternatively, they can also be acquired by using fitting with Eq. (B5).

Funding. Research Fund of Guangdong-Hong Kong-Macao Joint Laboratory for Intelligent Micro-Nano Optoelectronic Technology (2020B1212030010); National Natural Science Foundation of China (61307062).

Acknowledgment. We acknowledge financial support from the Research Fund of Guangdong-Hong Kong-Macao Joint Laboratory for Intelligent Micro-Nano Optoelectronic Technology and the National Natural Science Foundation of China. Su Zhi-Kun thanks Rong Hai-Wu and Qin Xi-Zhou for useful discussions.

Disclosures. The authors declare no conflicts of interest.

Data Availability. Data underlying the results presented in this paper are not publicly available at this time but may be obtained from the authors upon reasonable request.

REFERENCES

1. G. Stokes, "On the composition and resolution of streams of polarized light from different sources," Trans. Camb. Phil. Soc. **9**, 399–416 (1852).
2. D. Goldstein, *Polarized Light* (CRC Press, 2011).
3. R. Azzam, "Division-of-amplitude photopolarimeter (DOAP) for the simultaneous measurement of all four Stokes parameters of light," Opt. Acta **29**, 685–689 (1982).
4. R. Azzam, "Arrangement of four photodetectors for measuring the state of polarization of light," Opt. Lett. **10**, 309–311 (1985).
5. R. Azzam, I. Elminyawi, and A. El-Saba, "General analysis and optimization of the four-detector photopolarimeter," J. Opt. Soc. Am. A **5**, 681–689 (1988).
6. B. Schaefer, E. Collett, R. Smyth, D. Barrett, and B. Fraher, "Measuring the Stokes polarization parameters," Am. J. Phys. **2**, 163–168 (2007).
7. S. Lu, C. Zhang, and J. Han, "Research on measuring polarization state of light by stokes parameters based on electro optic effect," Appl. Opt. **54**, 4214–4220 (2015).
8. A. Kuma and A. Ghatak, *Polarization of Light with Applications in Optical Fibers* (SPIE Press, 2011).
9. R. Azzam, "Photopolarimetric measurement of the Mueller matrix by Fourier analysis of a single detected signal," Opt. Lett. **2**, 148–150 (1978).
10. R. Simon and N. Mukunda, "Minimual three-component Su(2) gadget for polarization optics," Phys. Lett. A **143**, 165–169 (1990).
11. U. Schilling, J. Zanthier, and G. Agarwal, "Measuring arbitrary-order coherence: tomography of sing-mode multiphoton polarization-entangled states," Phys. Rev. A **81**, 013826 (2010).
12. Y. Israel, I. Afek, S. Rosen, O. Ambar, and Y. Silberberg, "Experimental tomography of NOON states with large photon numbers," Phys. Rev. A **85**, 022115 (2012).
13. J. Sakurai, *Modern Quantum Mechanics* (Addison-Wesley Publishing Company, 1994).
14. O. Rodrigues, "Des lois géométriques qui régissent les déplacements d'un système solide dans l'espace, et de la variation des coordonnées provenant de ces déplacements considérés indépendamment des causes qui peuvent les produire," J. Math. Pures Appl. **5**, 380–440 (1840).
15. E. Lee and D. Messerschmidt, *Digital Communication* (Kluwer Academic, 1994).
16. N. K. Langford, "Encoding, manipulating and measuring quantum information in optics," (Ph.D. Universtiy of Queensland, 2007).
17. A. Lizana, I. Estévez, F. A. Torres-Ruiz, A. Peinado, C. Ramirez, and J. Campos, "Arbitrary state of polarization with customized degree of polarization generator," Opt. Lett. **40**, 3790–3793 (2015).
18. Origin Lab, "Global fit for different functions with shared parameters," https://www.originlab.com/doc/Tutorials/Multi-Functions-Global-Fitting.
19. X.-F. Qian, A. N. Vamivakas, and J. H. Eberly, "Entanglement limits duality and vice versa," Optica **5**, 942–947 (2018).